Quantitative evaluation of the octadecylamine-assisted bulk separation of semiconducting and metallic single-wall carbon nanotubes by resonance Raman spectroscopy

Ge. G. Samsonidze[a)]
Department of Electrical Engineering and Computer Science, Massachusetts Institute of Technology, Cambridge, Massachusetts 02139-4307

S. G. Chou
Department of Chemistry, Massachusetts Institute of Technology, Cambridge, Massachusetts 02139-4307

A. P. Santos and V. W. Brar
Department of Physics, Massachusetts Institute of Technology, Cambridge, Massachusetts 02139-4307

G. Dresselhaus
Francis Bitter Magnet Laboratory, Massachusetts Institute of Technology, Cambridge, Massachusetts 02139-4307

M. S. Dresselhaus and A. Selbst
Department of Electrical Engineering and Computer Science and Department of Physics, Massachusetts Institute of Technology, Cambridge, Massachusetts 02139-4307

A. K. Swan, M. S. Ünlü, and B. B. Goldberg[b)]
Department of Electrical and Computer Engineering, Boston University, Boston, Massachusetts 02215-1714

D. Chattopadhyay, S. N. Kim, and F. Papadimitrakopoulos
Nanomaterials Optoelectronics Laboratory, Department of Chemistry, Polymer Program, Institute of Materials Science, University of Connecticut, Storrs, Connecticut 06269-3136

The selective stabilization of octadecylamine (ODA) on semiconducting (S) single-wall carbon nanotubes (SWNTs) has been reported to provide a means for the bulk separation of S from metallic (M) SWNTs. Utilizing resonance Raman spectroscopy and, in particular, the relative changes in the integrated intensities of the radial-breathing mode region, a generic method has been developed to provide quantitative evaluation of the separation efficiency between M and S SWNTs along with diameter separation. The ODA-assisted separation is shown to provide S enrichment by a factor of 5 for SWNTs prepared by high pressure CO decomposition and greater S enrichment for SWNTs with diameters below 1 nm. © *2004 American Institute of Physics.* [DOI: 10.1063/1.1777814]

Within the family of one-dimensional (1D) materials, single-wall carbon nanotubes (SWNTs) play a major role because of their many unique properties,[1] whereby a SWNT can be either metallic (M) or semiconducting (S), depending only on its geometrical structure.[2,3] Presently available SWNT synthesis methods show no selectivity for M or S SWNTs, yielding a product that is a mixture of both M and S SWNTs. Postsynthesis separation of M and S SWNTs is thus of great interest for the SWNT research community. One of the recently reported separation mechanisms is attributed to the enhanced chemical affinity of the octadecylamine (ODA) surfactant for S SWNTs. The ODA exfoliates SWNT ropes to small bundles (containing two to six SWNTs) when dispersed in tetrahydrofuran (THF), rendering M-enriched bundles more prone to precipitation when the THF is partially evaporated.[4] Several other separation techniques have also been reported recently.[5–8]

These reports[4–8] use resonance Raman spectroscopy (RRS), among other methods, as proof of their separation of

M and S SWNTs, since RRS is a common tool for the characterization of SWNTs, both when arranged in bundles[9] and as isolated tubes.[10] However, the relative intensities of the RRS features associated with M and S SWNTs at one laser excitation energy do not reflect the proportions of the corresponding SWNTs in the sample.[11] The RRS intensities are resonantly enhanced when the laser excitation energy (E_{laser}) approximately matches one of the van Hove singularities (VHSs) in the joint density of electronic states (JDOS) of individual 1D SWNTs.[10] We thus need to consider both the SWNTs contained in the sample and the different resonance enhancement factors for each SWNT contributing to the Raman spectrum for several E_{laser}, in order to obtain the separation efficiency of M and S SWNTs. In this letter, we introduce a method for evaluating the ratio of M to S SWNTs in the different fractions of the separation process relative to their presence in the initial sample, using RRS at several E_{laser} values, based on several assumptions. An illustrative application of this method is made here to the ODA-assisted separation process[4] applied to SWNTs prepared by the high pressure CO decomposition (HiPco process).

Among the various features observed in the Raman spectra, the radial-breathing mode (RBM) is the most suitable for

---

[a)]Electronic mail: gsm@mgm.mit.edu
[b)]Also at: Department of Physics, Boston University, Boston, MA 02215-1714.

Appl. Phys. Lett., Vol. 85, No. 6, 9 August 2004

Samsonidze *et al.*   1007

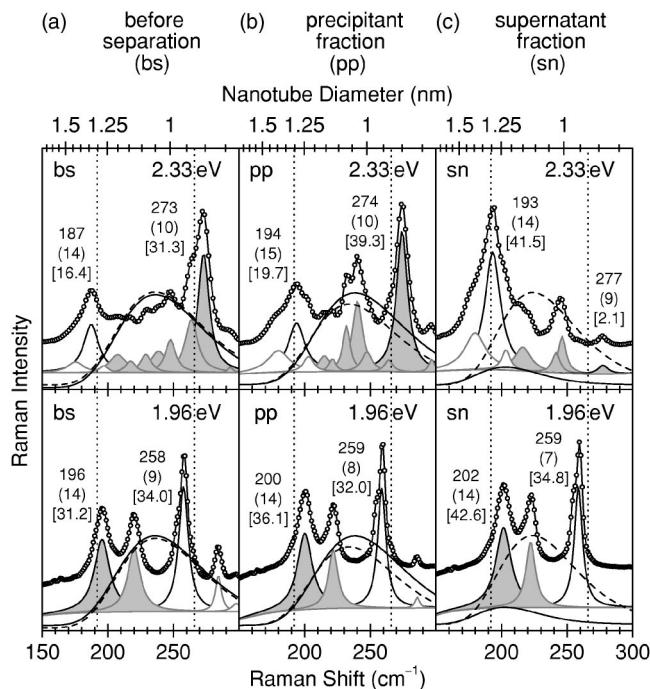FIG. 1. Open circles show RBM profiles at $E_{laser}=2.33$ eV (upper traces) and at $E_{laser}=1.96$ eV (lower traces) for the (a) "as-prepared" HiPco sample ps, and (b) pp (M enriched) and (c) sn (S enriched) fractions after the separation process. From the spectral line shape analysis, white and gray peaks show Lorentzians associated with S and M resonant SWNTs, respectively. Those Lorentzians surrounded by black borders are labeled by their mean frequency and full width of half maximum in cm^{-1}, and [area] in % (where 100% corresponds to the sum of all Lorentzian areas in the starting SWNT material (a) at a given E_{laser}). The d_t distributions are shown as functions of ω_{RBM} by solid (M) and dashed (S) lines. The vertical dotted lines show large ($\mathcal{L}$) and small (s) diameters, i.e., $d_t^{\mathcal{L}}=1.30$ nm and $d_t^s=0.93$ nm. The top scale links RBM frequencies to SWNT diameters.

TABLE I. The enrichment factors of M and S SWNTs of s and $\mathcal{L}$ diameters in the pp and sn fractions ($\mathcal{F}$) with respect to the bs material derived from the RBM features at $E_{laser}=2.33$ eV and 1.96 eV shown in Fig. 1, the (M:S) ratios and the mean diameters $\bar{d}_t^M$ and $\bar{d}_t^S$ (in nm) for M and S SWNTs in these fractions.

$\mathcal{F}$	Ms	$M\mathcal{L}$	Ss	$S\mathcal{L}$	(M:S)	$\bar{d}_t^M$	$\bar{d}_t^S$
pp	1.26	1.16	0.94	1.20	(1.14:2)	1.04	1.06
sn	0.07	1.37	1.02	2.53	(1:10.4)	1.23	1.11

RBMs for many laser lines.[15] Using these values for α and β, we can uniquely identify each Lorentzian with either M or S SWNTs from the Kataura plot, as shown in Fig. 1 in white (S) and gray (M), yet a specific (n,m) assignment of SWNTs is still an open issue. Note that $E_{laser}=2.33$ eV excites small d_t M SWNTs (higher RBM frequencies) and large d_t S SWNTs (lower RBM frequencies), while $E_{laser}=1.96$ eV does the opposite, exciting small d_t S SWNTs and large d_t M SWNTs.

The ratio of the number of M SWNTs to the number of S SWNTs in the sample, hereafter referred as the (M:S) ratio, can be found by approximating the d_t distributions for M and S SWNTs. The starting d_t distribution for both M and S SWNTs can be obtained from the RBM spectra shown in Fig. 1(a) following the state-of-the-art fitting procedure of Kuzmany, *et al.*[14] yielding 1.05 ± 0.15 nm (Gaussian with mean diameter $\bar{d}_t=1.05$ nm and variance $\sigma=0.15$ nm).[15] We assume here that the initial (M:S) ratio is (1:2), which is the commonly accepted value for randomly grown SWNT. However, different synthesis processes may yield (M:S) ratios that vary from this (1:2) value.[16]

To evaluate the d_t distributions for M and S SWNTs in the pp and sn fractions, we select the two Lorentzians near 192 and 266 cm^{-1} which are present in all spectra (shown by vertical dotted lines in Fig. 1), corresponding to larger ($\mathcal{L}$) [$d_t^{\mathcal{L}}=1.30$ nm] and smaller (s) [$d_t^s=0.93$ nm] diameter SWNTs, respectively. Note that the sampling diameters, d_t^s and $d_t^{\mathcal{L}}$, are chosen at opposite sides of $\bar{d}_t$, which is essential for distinguishing between the d_t separation and the (M:S) separation. The relative quantities of M and S SWNTs with s and $\mathcal{L}$ diameters in the pp and sn fractions with respect to the ps material (hereafter referred as the enrichment factors) are obtained by dividing the areas of the Lorentzians in Figs. 1(b) and 1(c) by the areas of the corresponding Lorentzians in Fig. 1(a), which allows us to eliminate the unknown resonance enhancement factors for the individual (n,m) SWNTs contributing to the spectra, thus avoiding a specific (n,m) assignment. It is essential that the RBM spectra for all the fractions (ps, pp, and sn) at a given E_{laser} are taken under the same experimental conditions (laser power, spectrum accumulation time, extent of SWNT bundling, etc.) to ensure proper normalization of the Lorentzian areas. For example, the enrichment factors for S SWNTs of $\mathcal{L}$ diameter (hereafter denoted by $S\mathcal{L}$) are given by $19.7/16.4=1.20$ and $41.5/16.4=2.53$ for the pp and sn fractions, respectively (see Lorentzian areas shown in Fig. 1). This ($S\mathcal{L}$) and other (Ms, $M\mathcal{L}$, and Ss) enrichment factors for the pp and sn fractions are summarized in Table I.

The enrichment factors provide information on the (M:S) separation in the pp and sn fractions, and also on the d_t separation, if any. If no d_t separation occurs, $Ms=M\mathcal{L}$ and

estimation of the separation efficiency of M and S being SWNTs. This is due to the RBM frequency (ω_{RBM}) being inversely proportional to the SWNT diameter (d_t),[12] and the M and S SWNTs with different d_t being resonant with a given E_{laser}[13] thereby distinguishing RBM features attributed to M SWNTs from those of S SWNTs. RBM profiles of an "as-prepared" HiPco sample before separation (ps), as well as the precipitant (pp), and supernatant (sn) fractions after separation, taken with $E_{laser}=2.33$ eV and 1.96 eV, are shown in Figs. 1(a)–1(c), respectively. The measurements were performed on ODA-dispersed SWNTs, drop casted on a Si/SiO$_2$ substrate, followed by removing the ODA surfactant by an extensive chloroform wash and an anneal it at 200 °C under vacuum, which results in bundled SWNTs.

Each Lorentzian from the line shape analysis with background subtraction (to 5% accuracy) shown in Fig. 1 arises from a superposition of several different (n,m) SWNTs that are resonant with E_{laser}, while most (n,m) SWNTs within the sample are not resonant and do not contribute to the RBM intensity. To identify the observed Lorentzian features with M or S SWNTs, we use a Kataura plot,[13] giving the VHS energies in the JDOS for all (n,m) SWNTs as a function of d_t. While the resonant VHSs in the Kataura plot are selected by E_{laser}, the d_t values are obtained from ω_{RBM} according to the relation $\omega_{RBM}=\alpha/d_t+\beta$.[14] The coefficients α and β are very sensitive to the SWNT synthesis method and SWNT surroundings.[14] For bundled HiPco SWNTs, we obtained $\alpha=239$ cm^{-1} nm and $\beta=8.5$ cm^{-1} we obtained by fitting

$Ss=S\mathcal{L}$ is expected, while if no $(M:S)$ separation occurs, $Ms=Ss$ and $M\mathcal{L}=S\mathcal{L}$ are anticipated. By comparing the enrichment factors listed in Table I, we see that none of these conditions is satisfied for our pp and sn fractions, thus implying that both $(M:S)$ separation and d_t separation take place simultaneously.

Information on the $(M:S)$ separation and the d_t separation stored in the enrichment factors (Ms, $M\mathcal{L}$, Ss, and $S\mathcal{L}$) is extracted by fitting the d_t distributions for M and S SWNTs in the pp and sn fractions to Gaussian functions. For each fraction, the two Gaussians for M and S SWNTs will generally have different amplitudes and different mean diameters, but the same variance as the starting SWNT material, $\sigma=0.15$ nm. The latter assumption is reasonable as long as the d_t separation is not too severe, as will be shown elsewhere.[17] We then solve for the four unknowns (amplitudes and mean diameters of M and S Gaussians) to fit the four enrichment factors. The $(M:S)$ ratio is then given by the ratio of the amplitudes of M and S Gaussians multiplied by the assumed $(1:2)$ ratio for the starting SWNT material. The former ratio of the Gaussian amplitudes is given by $\sqrt{(MsM\mathcal{L})/(SsS\mathcal{L})}$, that is the ratio of enrichment factors for M and S SWNTs averaged over s and $\mathcal{L}$ diameters.[17] Similarly, the mean diameters of M and S Gaussians, $\bar{d}_t^{\,M}$ and $\bar{d}_t^{\,S}$, are determined by the ratios of the enrichment factors for $\mathcal{L}$ and s diameters, $M\mathcal{L}/Ms$ and $S\mathcal{L}/Ss$. Namely, changes in the mean diameters $\bar{d}_t^{\,M}-\bar{d}_t$ and $\bar{d}_t^{\,S}-\bar{d}_t$ are equal to $\ln(M\mathcal{L}/Ms)$ and $\ln(S\mathcal{L}/Ss)$, respectively, multiplied by $\sigma^2/(d_t^{\mathcal{L}}-d_t^{\,s})$, as follows from fitting the Gaussians to the enrichment factor data.[17] The overall $(M:S)$ ratios and the mean diameters $\bar{d}_t^{\,M}$ and $\bar{d}_t^{\,s}$ thus calculated are summarized in Table I. The corresponding d_t distributions are plotted as functions of ω_{RBM} in the background of Fig. 1 by solid (M) and dashed (S) lines. Similar measurements performed on the same samples at a different pair of laser lines ($E_{laser}=2.41$ eV and 1.92 eV) suggest that the accuracy of the present analysis protocol is within 20%. See EPAPS Ref. 18 for supplemental material (Fig. S-1 and Table S-1).

According to the $(M:S)$ ratios listed in Table I, an overall enrichment of $10.4/2=5.1$ [or $10.4/(10.4+1)=91\%$ assuming a $(1:2)$ ratio in the ps material] was obtained for S SWNTs in the sn fraction, which is explained by the increased affinity of ODA toward S SWNTs, rendering S-enriched bundles more prone to remain in the sn fraction.[4] On the other hand, the M SWNTs in the pp fraction show a modest enrichment of only 14%, indicating precipitation of an adequate amount of S SWNTs in order to remove the bundles with high M-content, so that most SWNT material ends up in the pp fraction, while little is left in the sn fraction. However, as evident by comparing Ms and $M\mathcal{L}$ enrichment factors for the sn fraction (see Table I), the presence of a considerable amount of large d_t (above 1 nm) M SWNTs in the sn fraction lowers the overall $(M:S)$ ratio, that would otherwise be around $Ss/Ms=1.02/0.07=14.6$ [or $(M:S)=(1:29.2)$] for SWNTs of d_t below 1 nm. Similarly, poor enhancement results have been observed for the higher-diameter (1.37 ± 0.18 nm) laser-ablated SWNT samples.[4] The reasons behind this d_t dependence of the enrichment factors are not currently understood and might originate from either electronic amine–SWNT interactions or curvature-induced stabilization.

An analytic method is presented for evaluating the $(M:S)$ and d_t separation efficiencies, based on the line shape analysis of the RBM features in the RRS probed using two specially selected E_{laser}, which for this sample approximately take account of the d_t distribution. Explicit application to the recently developed ODA-assisted bulk SWNT separation process demonstrates that it is effective in generating fractions five times enriched in S SWNTs. Further improvement in separation efficiency is expected for SWNT samples with d_t distributions centered below 1 nm. Use of the RRS characterization method, which can also be applied and extended to other separation processes, can thus help to further advance the separation methodology. The evaluation method for the $(M:S)$ and d_t separations with multiple laser lines, which would further refine the analysis protocol, will be published in more detail elsewhere.[17]

[1] M. S. Dresselhaus, G. Dresselhaus, and P. Avouris, *Carbon Nanotubes: Synthesis, Structure, Properties and Applications*, Springer Series in Topics in Applied Physics Vol. 80. (Springer, Berlin, 2001).

[2] R. Saito, M. Fujita, G. Dresselhaus, and M. S. Dresselhaus, Appl. Phys. Lett. **60**, 2204 (1992).

[3] N. Hamada, S. Sawada, and A. Oshiyama, Phys. Rev. Lett. **68**, 1579 (1992).

[4] D. Chattopadhyay, I. Galeska, and F. Papadimitrakopoulos, J. Am. Chem. Soc. **125**, 3370 (2003).

[5] M. Zheng, A. Jagota, E. D. Semke, B. A. Diner, R. S. McLean, S. R. Lustig, R. E. Richardson, and N. G. Tassi, Nat. Mater. **2**, 338 (2003); M. Zheng, A. Jagota, M. S. Strano, A. P. Santos, P. Barone, S. G. Chou, B. A. Diner, M. S. Dresselhaus, R. S. McLean, G. B. Onoa, Ge. G. Samsonidze, E. D. Semke, M. Usrey, and D. J. Walls, Science **302**, 1545 (2003).

[6] R. Krupke, F. Hennrich, H. V. Löhneysen, and M. M. Kappes, Science **301**, 344 (2003).

[7] M. S. Strano, C. A. Dyke, M. L. Usrey, P. W. Barone, M. J. Allen, H. Shan, C. Kittrell, R. H. Hauge, J. M. Tour, and R. E. Smalley. Science **301**, 1519 (2003).

[8] Z. Chen, X. Du, M.-H. Du, C. D. Rancken, H.-P. Cheng, and A. G. Rinzler. Nano Lett. **3**, 1245 (2003).

[9] M. S. Dresselhaus and P. C. Eklund, Adv. Phys. **49**, 705 (2000).

[10] M. S. Dresselhaus, G. Dresselhaus, A. Jorio, A. G. Souza Filho, and R. Saito, Carbon **40**, 2043 (2002).

[11] P.-H. Tan, Y. Tang, C. Y. Hu, F. Li, Y. L. Wei, and H. M. Cheng, Phys. Rev. B **62**, 5186 (2000).

[12] J. Kürti, G. Kresse, and H. Kuzmany, Phys. Rev. B **58**, R8869 (1998).

[13] H. Kataura, Y. Kumazawa, Y. Maniwa, I. Uemezu, S. Suzuki, Y. Ohtsuka, and Y. Achiba, Synth. Met. **103**, 2555 (1999).

[14] H. Kuzmany, W. Plank, M. Hulman, C. Kramberger, A. Grüneis, T. Pichler, H. Peterlik, H. Kataura, and Y. Achiba, Eur. Phys. J. B **22**, 307 (2001).

[15] A. Kukovecz, C. Kramberger, V. Georgakilas, M. Prato, and H. Kuzmany, Eur. Phys. J. B **28**, 223 (2002).

[16] Y. Li, D. Mann, M. Rolandi, W. Kim, A. Ural, S. Hung, A. Javey, J. Cao, D. Wang, E. Yenilmez, Q. Wang, J. F. Gibbons, Y. Nishi, and H. Dai, Nano Lett. **4**, 317 (2004).

[17] V. W. Brar, Ge. G. Samsonidze, A. P. Santos, S. G. Chou, D. Chattopadhyay, S. N. Kim, F. Papadimitrakopoulos, M. Zheng, A. Jagota, G. B. Onoa, A. K. Swan, M. S. Ünlü, B. B. Goldberg, G. Dresselhaus, and M. S. Dresselhaus, J. Nanosci. Nanotechnol. (in press).

[18] See EPAPS Document No. E-APPLAB-85-010431 for supplemental material. A direct link to this document may be found in the online article's HTML reference section. The document may be reached via the EPAPS homepage (http://www.aip.org/pubservs/epaps.html) or from ft-p.aip.org in the directory /epaps/. See the EPAPS homepage for more information.